OPTIMIZATION OF BLADE PROFILE FOR GOVERNING STAGE IN PEAK REGULATING CONDITION

Pan LI[1*]，Kai SONG[1]，Haichao PENG[2]，Heyong SI[1]

1. School of Energy and Power Engineering, Northeast Electric Power University, Jilin, China;
2. State Grid Songyuan Elect Power Supply Co, Jilin, China

Blade loss seriously affects the stage efficiency of steam turbine. The Genetic Algorithm is used to optimize the NURBS curve of blade profile in governing stage. With the maximum value of the function composed of total pressure loss coefficient, steam flow Angle and static pressure ratio, the optimized blade profile in peak regulating condition is obtained. The flow pattern of internal flow field, the load distribution of blade and the development law of cascade losses are studied before and after blade profile optimization. The results show that after blade profile optimization, larger rotor blade leading edge diameter can effectively reduce the influence of steam attack angle on the flow field when the volume flow rate is small. The smoother suction surface and thinner trailing edge can reduce the end wall loss in the cascade passage, which leads to the reduction of the influence area of secondary flow, the effective restraint of the boundary layer thickness on the blade surface, the reduction of blade loss, and the improvement of flow efficiency of the governing stage after optimization. The optimized blade not only improves the performance in the peak regulating condition, but also has good performance in the design condition.

Key words: *steam turbine; governing stage; optimization; genetic algorithm; numerical simulation.*

1.Introduction

In order to meet the demand of power peak regulation, the thermal power generating units often operate at low load, and the main equipment of thermal power generating units is not designed for low load conditions, which causes huge deviation between the main operating parameters and the design parameters of the generating units under low load conditions, and also causes significant increase in the energy consumption of the generating units. For steam turbine, the efficiency of the governing stage and the last stage decrease most significantly. When operating under high temperature and high-pressure conditions, the governing stage whose blades have a relatively small aspect ratio will suffer great blade losses and end wall losses. Such losses will increase under the working conditions of low load and small volume flow rate. As a result, the stage efficiency will further decrease. Therefore, improving the efficiency of the governing stage under peak regulation conditions can help improve the peak regulation capacity of large thermal power generating units, thus making it more flexible to

*Corresponding author; E-mail:283395346@qq.com

regulate the power grid.

In order to improve the efficiency of the governing stage under deep peak load condition, the blade profile of the governing stage with good performance should be designed. In the optimization design of blade profile, automatic optimization method has attracted more and more attention [1]. This method which combines optimization technology with flow field calculation can make the design process more objective [2]. The automatic optimization method is to try to parameterize the existing blade profile, that is, to describe the blade profile data by several important blade profile design parameters. At present, there are many published parameterization methods of blade profile, among which the construction method [3] is more common. The construction method is to describe the accurate blade profile data by constructing function curves. The such common methods include polynomial parameterization [4], B-Spline line parameterization [5], Bezier line parameterization [6] and NURBS line parameterization [7]. Cheng Jinxin et al. [8] used multi-section Bezier curves to reconstruct the characteristic lines of S1 flow surface to parameterize the blade profile of axial compressor blades. Cheng Yan et al. [9] developed an efficient integrated design optimization approach explicitly tailored for the aerodynamic optimization of turbine blade profiles, which combines the Particle Swarm Optimization with a Bezier curves parametric modeling technique of turbine blades and high-fidelity CFD simulation analysis. Georgia et al. [10] proposed that arc and thickness distribution in NURBS curve construction be used to realize parameterization of blade profile. In terms of automatic optimization technology, most researchers adopt numerical optimization method based on Genetic Algorithm to optimize the blade design, and the designed blade can not only maintain superior performance under design conditions, but also still perform well under off-design conditions. Wang Wei et al. [11] introduced entropy production theory into the optimal design of two-dimensional blade profiles, and combined genetic algorithm with Navier-Stokes equation solving technology to propose a method that can accurately quantify aerodynamic loss at any position of cascade, which has been well verified in the design. Song P et al. [12] adopted an optimization platform based on the combination of genetic algorithm and CFD to carry out two-dimensional aerodynamic optimization of the stator blade profile, pointing out that the load area of the trailing edge can effectively inhibit the development of the boundary layer on the cascade surface, and the optimized blade profile has also achieved good design results. Yu Jia et al. [13] made use of Genetic Algorithm by parameterizing the profiles of two-dimensional blades at different spanwise heights of the blades of a multi-stage axial compressor to obtain significant gains in performance. Yang Jutao et al. [14] proposed an optimization process to design the baseline rotor of a supersonic through flow fan (STFF) at an inlet Mach number of 2.0 based on Genetic Algorithm. The performance of the rotor of the STFF that was reconstructed by stacking the optimized elements of the blade was improved at the design point as well as in off-design conditions by using three-dimensional computational fluid dynamics (CFD) simulations.

In this paper, the iterative optimization theory of genetic algorithm is applied to the NURBS curve optimization of the parameterized blade profile, and the optimized blade profile with good performance is obtained under the small volume flow condition. In addition, the steady numerical simulation of the stage flow field before and after profile optimization is carried out by using CFD method to verify the flow field effect of blade profile optimization, and to explore the influence of profile parameters on the blade loss in cascades.

2. Numerical Optimization Method

2.1 Parameterization method of blade profile

The purpose of constructing the blade profile by NURBS curve is to solve the NURBS curve equations by several important basic blade design parameters. The expressions of the NURBS curve equations are as follows:

$$P(u)=\sum_{i=0}^{n}V_iR_{i,k}(u) \tag{1}$$

$$R_{i,k}(u)=\frac{W_iB_{i,k}(u)}{\sum_{j=0}^{n}W_jB_{j,k}(u)} \tag{2}$$

Where $R_{i,k}(u)$ is the rational basis function, V_i represents the i th geometric control point, W_i is the weight of the control point, and $B_{i,k}(u)$ is the basis function of the k-degree B-spline.

$$\left.\begin{aligned} &B_{i,0}(u)=1 && u_i\le u\le u_{i+1}\\ &B_{i,0}(u)=0 && others\\ &B_{i,k}(u)=\frac{u-u_i}{u_{i+k}-u_i}B_{i,k-1}(u)+\\ &\frac{u_{i+k+1}-u}{u_{i+k+1}-u_{i+1}}B_{i+1,k-1}(u) && k\ge 1 \end{aligned}\right\} \tag{3}$$

Where u_i represents a B-spline node and u is a variable. In order to ensure that the curve passes through the first and last geometric control points, for k-order B-spline basis functions, there are $k+1$ nodes at each end of the node vector.

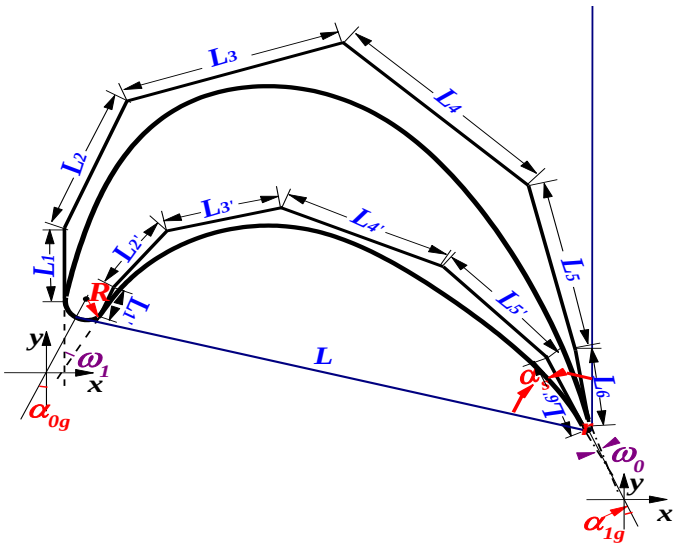

Fig. 1 Parameters of blade profile

In this paper, two NURBS curves of three degrees are used to describe two dimensional blade profile of governing stage blades. A total of 20 blade parameters were selected to construct the NUBRS curve. As shown in Fig.1, the selected blade design parameters are as follows: the chord length L, the blade installation Angle α_s, the geometric inlet Angle α_{0g}, the geometric outlet Angle α_{1g}, the leading edge inner tangential circle radius R, the trailing edge inner tangential circle radius r, the

leading edge tangent wedge Angle ω_1 and the trailing edge tangent wedge Angle ω_0. Meanwhile, the 12 side lengths of control polygons were also selected, which named L_1, L_2, L_3, L_4, L_5, L_6, $L_{1'}$, $L_{2'}$, $L_{3'}$, $L_{4'}$, $L_{5'}$ and $L_{6'}$. Among these parameters, the L and α_s can determine the axial length of blade. The R, α_{0g} and ω_1 are used to determine the starting point of two NURBS curves. The r, α_{1g} and ω_0 are used to determine the ending point of two NURBS curves. The length of L_1, L_2, $L_{1'}$ and $L_{2'}$ can affect the continuity of the leading edge. The length of L_5, L_6, $L_{5'}$ and $L_{6'}$ can affect the continuity of the trailing edge. The length of L_3, L_4, $L_{3'}$and $L_{4'}$ can affect the thickness of the blade. Based on this, the NURBS curves are well described by the 20 blade profile parameters.

2.2 Genetic algorithm optimization strategy

Genetic algorithm (GA) is an optimization method developed from Darwin's natural selection mechanism. Because of the ergodic nature of the evolution process, it is more suitable for global optimization of multiple problems. In order to ensure the strength and bearing capacity of the optimized blade, the axial length and maximum thickness of the blade should be kept unchanged. Therefore, the L, α_s, L_3, L_4, $L_{3'}$ and $L_{4'}$ should be consistent with the pre-optimization blade profile. In the Genetic Algorithm, six blade design parameters (α_{0g}、α_{1g}、R、r、ω_1，ω_0) and eight parameters of the NURBS curve control polygon side length (L_1、$L_{1'}$、L_2、$L_{2'}$、L_5、$L_{5'}$、L_6，$L_{6'}$) were selected as the basic variables. The variable range of these base variables are shown in Table 1. According to the requirements of blade profile design, the basic variables were coded after given the variable range.

The formulation of the objective function plays an important role in the optimization of the blade profile. In peak regulation, it is required that the regulating stage should maintain high efficiency even under low flow condition. However, the design parameters of the regulating stage can't reflect the performance of the whole flow condition. According to the above optimization purposes, the objective function should include the total pressure loss coefficient, the range of attack Angle that can adapt to the low flow condition and the parameters that can reflect the pressure ratio. Based on this, the biological evolution process is simulated with the total pressure loss coefficient, steam flow Angle and static pressure ratio in 30% load condition as the optimization objectives. The encoded variables were repeatedly selected, crossed and mutated. Each individual was evaluated according to the fitness function. The population was continuously evolved into a better group by elimination and selection.

Table 1 The variable range of base variables

Parameter	α_{0g}[°]	α_{1g}[°]	R [mm]	r[mm]	ω_1[°]	ω_0[°]	L_1[mm]
Stator	80-100	10-14	1.5-3.5	0.05-0.4	90-125	10-30	0.5-3
Rotor	18-33	16-19	1.5-3.5	0.05-0.4	80-100	15-35	0.5-3
Parameter	L_2[mm]	L_5[mm]	L_6[mm]	$L_{1'}$[mm]	$L_{2'}$[mm]	$L_{5'}$[mm]	$L_{6'}$[mm]
Stator	4-8	18-21	12-16	0.5-3	4-8	12-18	5-9
Rotor	10-16	33-36	14-18	0.1-3	6-10	12-18	4-8

The multi-objective function can be converted into a single objective function by the weight coefficient, and the formula is as follows:

$$F = 10 - c_1\omega - c_2\frac{\left|\Delta\beta - \Delta\beta_0\right|}{\Delta\beta_0} - c_3\frac{\left|\Delta p - \Delta p_0\right|}{\Delta p_0} \tag{4}$$

In the formula, c_1, c_2 and c_3 are the weight coefficients of the objective function, ω is the total pressure loss coefficient, $\Delta\beta$ and $\Delta\beta_0$ are respectively the steam flow Angle and the target steam flow Angle under small flow condition, Δp and Δp_0 are respectively the pressure ratio and the target pressure ratio under small flow condition.

According to equation (4), when the total pressure loss coefficient is minimum, the steam flow Angle reach the target value and the pressure ratio is also stable, the objective function will achieve the maximum value. The corresponding blade profile would be the optimal blade profile.

2.3 Computing method of 2D flow field

In order to shorten the calculation time, Navier-Stokes equations in any curve-coordinate system, finite volume space discretization and four-step Runge-Kutta time propulsion method were adopted to solve the results in the calculation program. Baldwin-Lomax model (B-L) was adopted for turbulence model. H-shaped grid with orthogonal wall surfaces was adopted, and the grid near the wall was appropriately increased in the number of layers. The number of nodes in the flow field calculation grid is about 55(horizontal direction) ×175(flow direction). The divided grid structure is shown in Fig. 2.

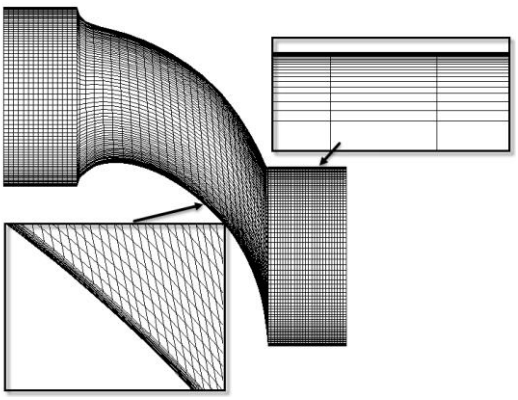

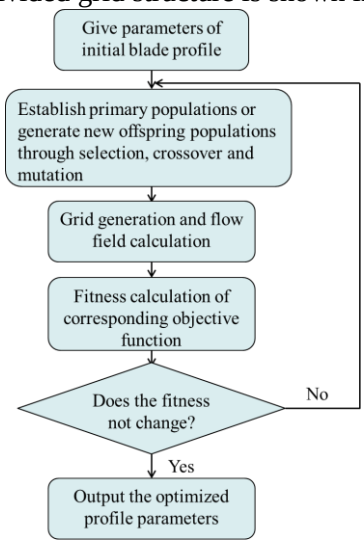

Fig. 2 Grid structure of model **Fig.3 Process of numerical optimization method**

In order to balance the contradiction between population diversity and computational efficiency, the number of populations is generally between 20 and 100. After the calculation and verification of different population numbers, it is determined that the population number is 60. The maximum number of generations is 50. After repeated verification, the operator of crossover is 0.75 and the operator of mutation is 0.02. The population reaches the maximum fitness of the objective function in about 22 generations. The calculation has good repeatability, and the maximum value of the objective function can be the same after many calculations. The average optimization time is about 100 hours. The overall calculation process is shown in Fig. 3.

The optimized blade profile generated according to each parameter is shown in Fig. 4. It can be seen from the figure that the optimized blade has a larger leading edge radius, a smoother back arc and a thinner trailing edge.

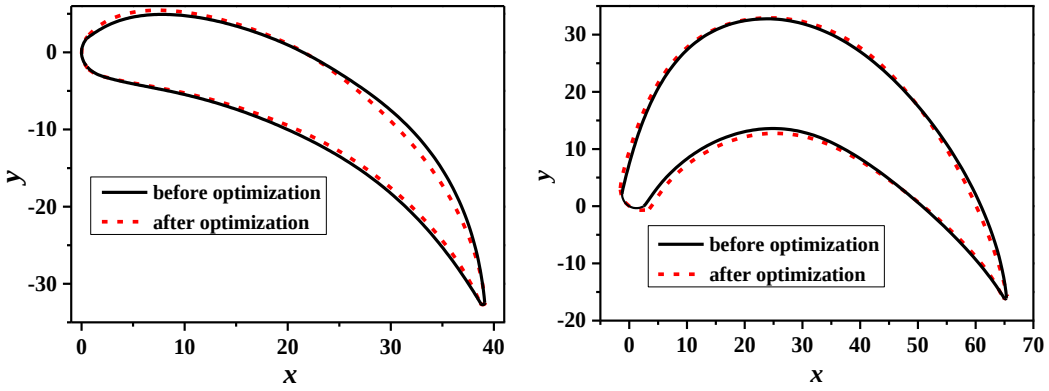

(a) stator (b) rotor

Fig.4 Comparison before and after blade profile optimization

3. Three-dimensional Numerical Calculation Method

3.1 Calculation model

In order to verify the effect of blade profile optimization, The Fluent software was used to simulate the three-dimensional steady flow field before and after optimization in the governing stage. Because the governing stage is usually composed of straight blades with constant cross-section, the 3D geometric model can be generated directly generated by stacking 2D blade profile lines along blade height. Fig. 5 shows the 3D geometric model of governing stage and its corresponding calculation grid. The model includes an extension section at the entrance of the stator, a stator passage section, a rotor passage section and an extension section at the exit of the rotor. High quality hexahedral meshes were used for the calculation. As shown in Fig. 5, boundary layer meshes were set along the profile lines of the stator blade and the rotor blade, and the wall meshes were also precisely processed to ensure the calculation accuracy. In addition, isentropic efficiency and total pressure loss coefficient are selected to verify the independence of the grid. As can be seen in Fig. 6, when the grid reaches 1.4 million, the monitored parameters are no longer sensitive to the number of grids. Therefore, the number of grids is divided as follows: 0.65 million in the stator passage and 0.75 million in the rotor passage. The total number of grids is about 1.4 million.

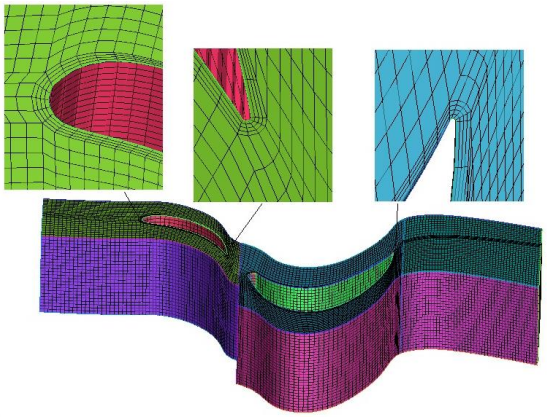

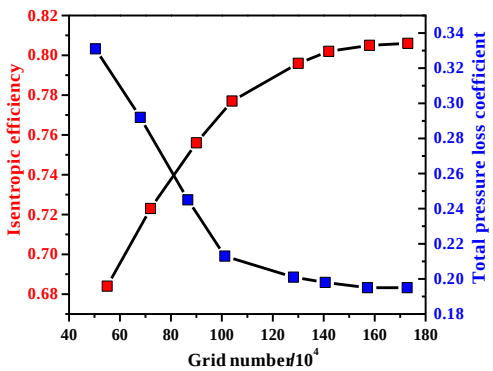

Fig.5 3D computational models and grids **Fig. 6. Dependence verification of grid number**

3.2 Boundary conditions

Superheated steam was used as the working medium for the numerical calculation. The inlet boundary of the model is set as the pressure inlet, and the outlet boundary is set as the pressure outlet. The setting values of inlet pressure, inlet temperature, outlet pressure and the flow rate under different load conditions are shown in Table 2. The circumferential surfaces are set as the periodic boundary of rotation. The surfaces of blade and hub are set to rotatable adiabatic wall condition and the speed are set to 3000 r/min.

Table 2 Steam parameters of governing stage under different loads

Load condition [%]	Inlet pressure [MPa]	Inlet temperature [K]	Outlet pressure [MPa]	flow rate [kgs^{-1}]
30	6.67	765.15	3.636	278.8
50	11.11	786.15	6.06	462
75	16.67	810.15	9.09	585
100	16.67	810.15	12.12	681

3.3 Numerical method

The finite-volume method is adopted for numerical calculation, the second-order upwind scheme is selected for spatial discretization, and the SIMPIE algorithm is used to accelerate the convergence. In order to select the correct turbulence model, several different turbulence models were selected for numerical simulation using the same boundary conditions as the experiments in literature [15]. The comparison between simulation results and experimental results is shown in Fig.7. The turbulence models are standard k-ε model, Renormalization-group k-ε (RNG k-ε) model, B-L model and shear stress transport (SST) model, respectively. Each model has its own advantages, but no universal model has been suggested.

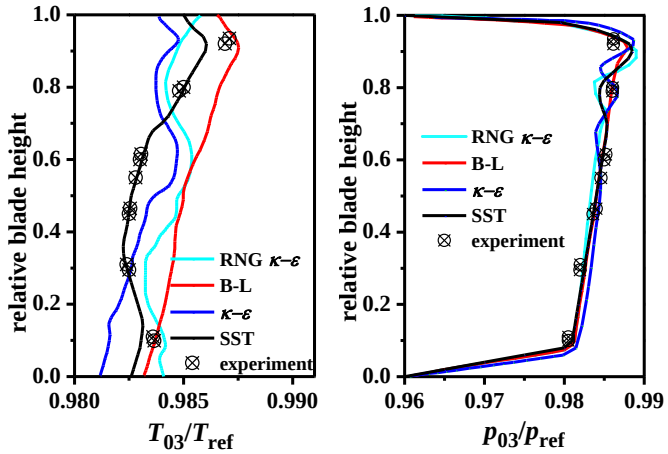

(a) temperature ratio (b) pressure ratio

Fig.7 Calculation result verification

The Fig.7 shows the distribution of pressure ratio and temperature ratio along the relative blade height at the model outlet. It can be seen that B-L model can better determine the distribution of pressure, but not accurate enough to estimate the friction resistance and temperature. Since the objective function of 2D profile optimization is concerned with the pressure distribution, B-L model can usually give satisfactory results. However, this model no longer works in 3D simulations. In contrast, the simulation value of SST turbulence model is in better agreement with the experimental

value, and the deviation is within the allowable range. So the SST turbulence model is chosen in the calculation to close the Reynolds mean equations. When the calculated residual is less than the order of 10^{-5}, the calculation is considered to be convergent.

4. Analysis of Results

4.1 Comparative analysis of blade performance under low load conditions

Fig. 8 shows the comparison of streamline distribution at roots of rotor blades before and after optimization. As can be seen in Fig. 8 (a), a vortex is formed near the wall at the front of the pressure surface before optimization. Due to the smaller leading-edge diameter of the rotor blade and the larger attack Angle of flow at the inlet of rotor under small volume flow, the rotor blade is more sensitive to the change of attack Angle before optimization, and the stationary point of the leading edge will move to the direction of the suction surface. As a result, the overexpansion of the pressure surface at the inlet of the rotor is aggravated, the reverse pressure gradient is increased, and the boundary layer is thickened. The low-energy fluid in boundary layer which is suppressed in the front of the pressure surface by the mainstream forms a vortex.

As shown in Fig. 8 (b), the leading edge diameter of the rotor blade becomes larger and is no longer sensitive to the change of the attack Angle after optimization. The low-energy fluid at the blade root will expand along the pressure gradient after bypassing the leading edge from the stationary point, and there is no reverse pressure gradient section. Therefore, the increased thickness of the boundary layer at the inlet of the rotor has little influence on the flow of the following part, and vortices no longer appear near the front wall of the blade pressure surface, thus improving the flow performance at the blade root.

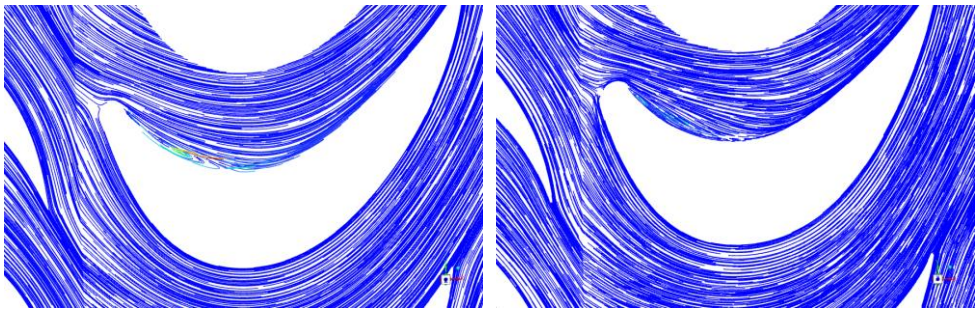

(a) before optimization (b) after optimization

Fig.8 Flow line distribution at the root of rotor blade

4.2 Comparative analysis of blade performance under low load conditions

Fig. 9 shows the energy loss coefficient of the cross section of rotor passage before and after optimization. The energy loss coefficient is defined as:

$$\omega = \frac{\left(p/p^*\right)^{\frac{\gamma-1}{\gamma}} - \left(p/p_0^*\right)^{\frac{\gamma-1}{\gamma}}}{1-\left(p/p_0^*\right)^{\frac{\gamma-1}{\gamma}}} \tag{5}$$

Where p_0^* is the average total pressure at the inlet of the stage, p^* is the relative local total pressure, p is the local static pressure, and γ is the adiabatic index with a value of 1.3.

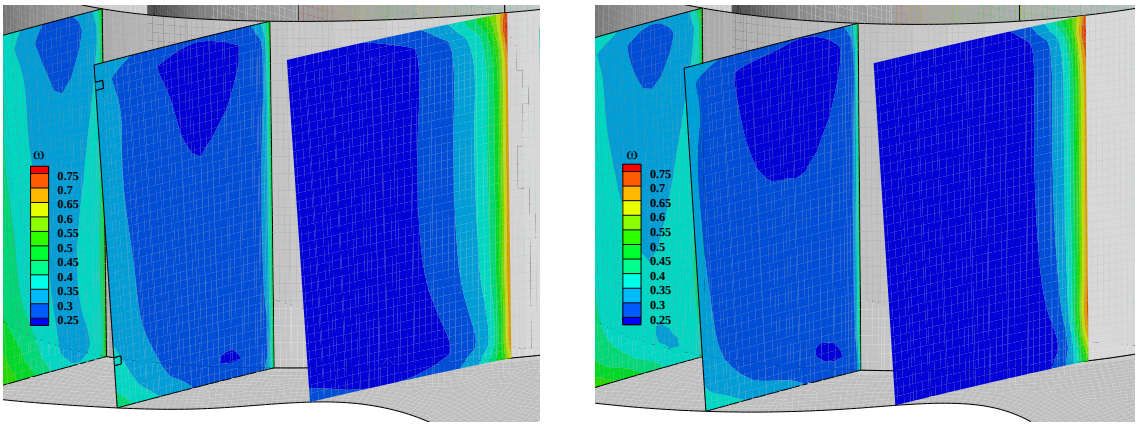

(a) before optimization (b) after optimization

Fig.9 Energy loss coefficient of rotor blade passage section

The energy loss coefficient increases at the trailing edge of the rotor blade. This indicates that the boundary layer will gradually thicken with the flow, and the low-energy fluid will gradually accumulate in the suction surface. The energy loss coefficient near the exit of the rotor is relatively high, and the flow loss will also increase.

Compared with Fig. 9 (a) and Fig. 9 (b), it can be seen that the energy loss coefficient of the section at the rear of the blade has reduced, and the boundary layer has decreased significantly after optimization. This is because the loading capacity of the optimized blade profile is improved. The pressure drop is mainly located in the rear part of the blade. In this way, the velocity of the steam flow in the rear part of the mainstream area is increased. Thus, the thickening of the rear boundary layer of the blade surface is inhibited and the flow loss is better reduced.

4.3 Analysis of blade performance in stage under different working conditions

Fig. 10 compares the blade surface pressure distribution of the governing stage before and after optimization. As can be seen in Fig. 10 (a), for the stator blade, the load of blade is increased and the loading capacity is improved after optimization at 30% load condition. The pressure drop is mainly located in the rear part of the blade, where the speed of the steam flow increases rapidly, thus inhibiting the thickening of the rear boundary layer of the blade surface after optimization. For the rotor blade, the pressure surface of the leading edge has a reverse pressure gradient due to the influence of the Angle of attack before optimization. But there is no inverse pressure gradient on the pressure surface of the leading edge after optimization. It is shown that the larger leading edge diameter can effectively reduce the influence of attack angle under small flow rate.

At 50% load condition, as shown in Fig. 10 (b), the blade surface pressure distribution trend is basically the same as under 30% load condition, indicating that the optimized blade also has good performance under this condition. At 100% load condition, as shown in Fig. 10 (c) , the pressure distribution at the leading edge of rotor blade are basically the same before and after optimization. But reverse pressure gradient appeared in the middle of the suction surface of the rotor blade, resulting in a certain flow loss before optimization. However, the steam flow is squeezed downward by the shape of the suction endwall after optimization. The pressure of the suction surface can be faired down and the reverse pressure gradient disappears, thus better reducing the flow loss.

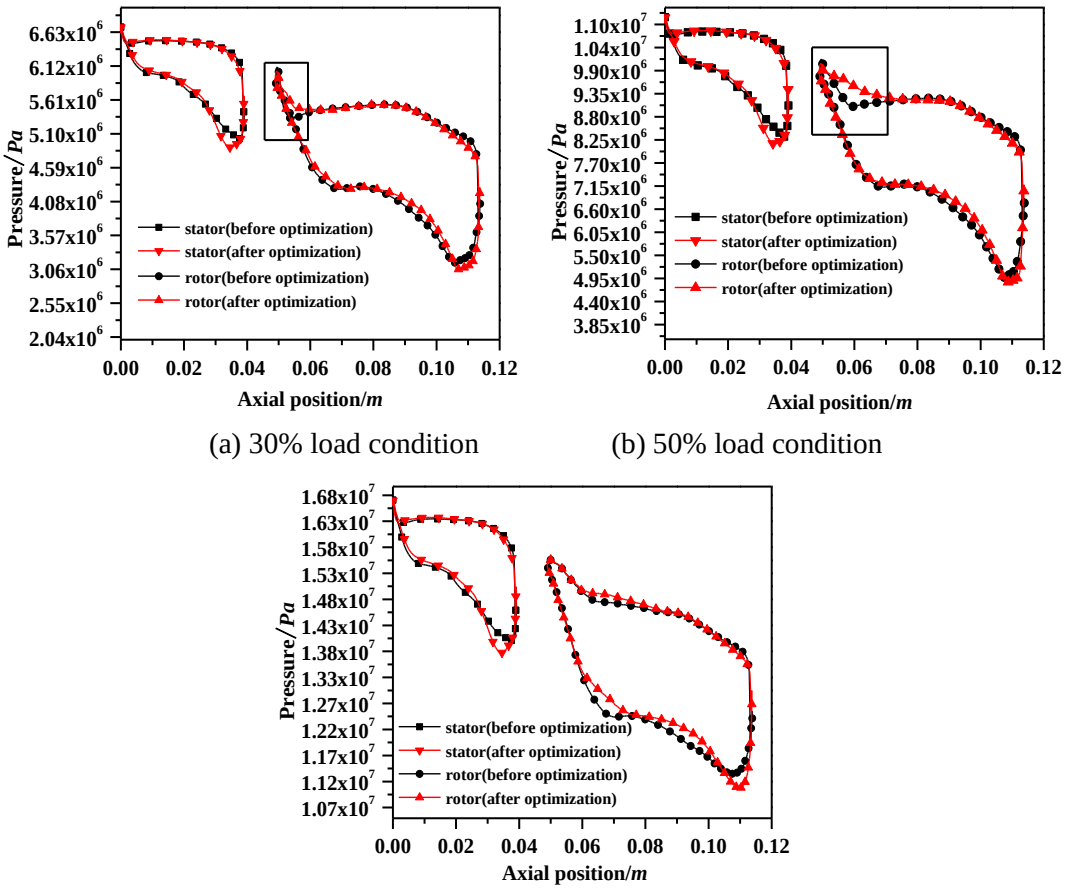

(a) 30% load condition (b) 50% load condition

(c) 100% load condition

Fig.10 Blade surface pressure distribution before and after optimization

In blade profile optimization, the flow loss of turbomachinery is mainly measured by parameters such as efficiency, total pressure loss or entropy increase. Since entropy increase is the only accurate measure of loss independent of reference system, the entropy increase is chosen to characterize flow-induced loss. The formula for entropy increase is as follows:

$$\Delta S_{\mathrm{l}} = \frac{C_p}{\gamma} \cdot \ln\left[\left(\frac{p_{\text{rotor-out}}}{p_{\text{stator-in}}}\right)^{(1-\gamma)}\left(\frac{T_{\text{rotor-out}}}{T_{\text{stator-in}}}\right)^{\gamma}\right] \tag{6}$$

Where C_{p} is the isobaric specific heat capacity; γ is the adiabatic index, taking the value as 1.3 for superheated steam; $p_{\text{rotor-out}}$ and $T_{\text{rotor-out}}$ are the pressure and temperature of the rotor outlet; $p_{\text{stator-in}}$ and $T_{\text{stator-in}}$ are the pressure and temperature of the stator inlet, respectively.

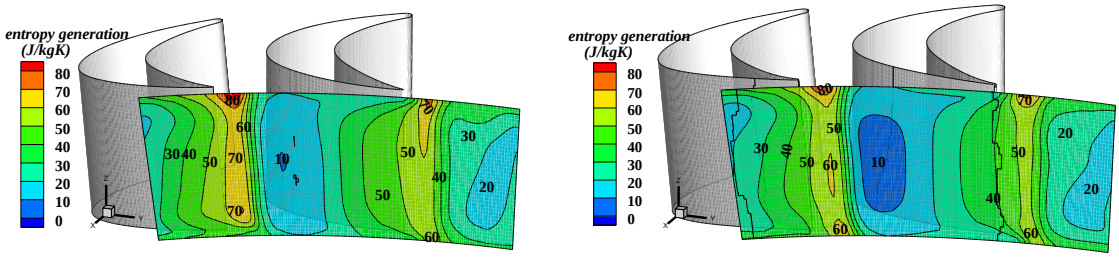

(a) before optimization (b) after optimization

Fig.11 Distribution of entropy increase at cascade outlet under 30% load condition

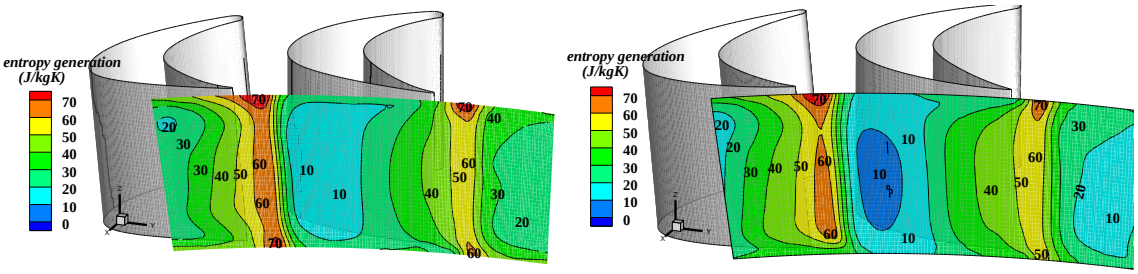

(a) before optimization (b) after optimization

Fig.12 Distribution of entropy increase at cascade outlet under 50% load condition

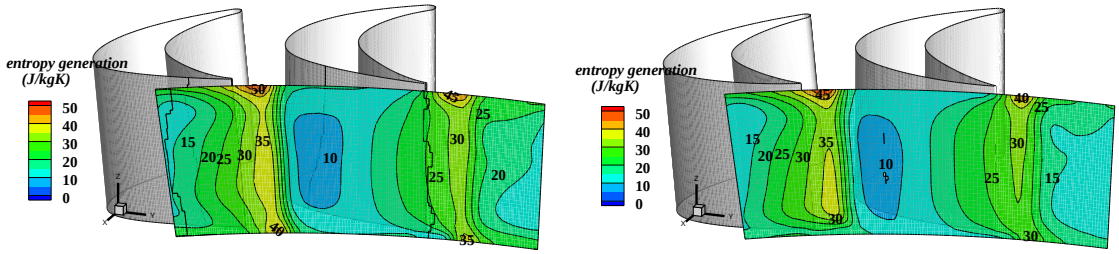

(a) before optimization (b) after optimization

Fig. 13 Distribution of entropy increase at cascade outlet under 100% load condition

It can be seen from Fig. 11 to Fig. 13 that the location where entropy increases the most at the cascade exit is in the wake region. The wake region is composed of low energy boundary layer fluid flowing from the suction surface and vortex shedding from the outlet. The flow loss across the wake region increases and decreases abruptly, but the peak value of loss is basically near the center of the wake region. The greatest loss occurs at the tip of the blade in the center of the wake region, which also contains secondary flow loss at the end wall. In short, the wake zone contains almost all flow loss around the flow profile.

As shown in Fig. 11, under 30% load condition, the peak region of wake loss decreases after optimization, and the entropy increase at the tip of the blade also tends to decrease. This is because the curvature of the suction-blade profile increases after optimization. This results in a thinner trailing edge, and improves loading capacity of the latter half of the blade. At the same time, the larger leading edge diameter and the thinner exit edge also reduce the secondary flow loss of the endwall in the blade cascade with large turning angle.

As shown in Fig. 12 and Fig. 13, under 50% and 100% load condition, the peak region of wake loss of the optimized blade profile also decreases, indicating that the flow loss is also effectively controlled under the conditions. At the same time, the secondary flow loss at the tip of the blade is also significantly reduced.

Table 3 shows the overall aerodynamic performance of the governing stage before and after optimization. After optimizing the blade profile of the governing stage through Genetic Algorithm, the isentropic efficiency of the governing stage is improved not only in the small flow condition, but also in other conditions. Within the calculated range, the maximum isentropic efficiency is increased by 1.66% under 30% load condition. Under the 100% load condition, the isentropic efficiency of the governing stage is also increased by 0.87%. It is indicated that the adaptability of the governing stage

to the operating conditions is improved after the blade optimization, which can also further improve the peak load regulation capacity of the unit.

Table 3 Comparison of isentropic efficiency before and after profile optimization

Parameters	isentropic efficiency[%]			
	100% load condition	75% load condition	50% load condition	30% load condition
Before optimization	90.80	90.20	83.46	78.26
After optimization	91.67	90.85	84.71	79.92

4. Conclusions

(1) The numerical optimization method based on the Genetic Algorithm can be used to optimize the NURBS curve of the blade profile of the governing stage, which can realize the optimization of the blade profile, and significantly improve the cascade performance after optimization.

(2) After optimization, the larger leading edge diameter can restrain the low energy flow and improve the performance of the rotor blades. The smoother back arc and thinner trailing edge can reduce the end wall loss in the blade passage of the governing stage and increase the load of the blade, effectively inhibit the boundary layer thickness on the blade surface, reduce blade profile loss, and improve flow efficiency.

(3) After optimizing the blade profile of the governing stage by the Genetic Algorithm, the isentropic efficiency of the governing stage increases by 1.66% and 0.87% at the small flow condition and the design condition respectively, and has different degrees of improvement in other operating conditions. The optimization of the blade profile can further improve the peak load capability of the steam turbine unit.

Nomenclature

C_p	–isobaric specific heat capacity, [Jkg^{-1}K^{-1}]	***Greek symbols***	
n	–rotation speed, [rmin^{-1}]	γ	–adiabatic index, [–]
$P(p)$	–pressure, [Pa]	ρ	–density, [kgm^{-3}]
T	–temperature, [K]	μ	–dynamic viscosity, [Nsm^{-2}]
u	–variable, [–]	ω	–total pressure loss coefficient, [–]

5. References

[1] Oyama, A., *et al.*, Transonic axial-flow blade optimization: evolutionary algorithms and three-dimensional Navier-Stokes solver, *Journal of Propulsion & Power*, 20(2012), 4, pp. 612-619

[2] Danish, S. N., *et al.*, Effect of tip clearance and rotor–stator axial gap on the efficiency of a multistage compressor, *Applied Thermal Engineering*, 99(2016), pp. 988-995

[3] Masters, D. A., *et al.*, Geometric comparison of aerofoil shape parameterization methods, 53rd *AIAA Journal*, 55(2015), 5, pp. 1575-1589

[4] Obayashi, S., *et al.*, Multi-objective genetic algorithm applied to aerodynamic design of cascade airfoils. *IEEE Transactions on Industrial Electronics*, 47(2000), 1, pp. 211-216
[5] Chao, S. M., *et al*., Optimization of a total internal reflection lens by using a hybrid Taguchi-simulated annealing algorithm, *Optical Review*, 21(2014), 2, pp. 153-161
[6] Li, H. L., *et al*.,. State variable and optimization potential-based multi-objective optimization method and application in compressor blade airfoil design, *Structural and Multidisciplinary Optimization*, 66(2023), 7, pp. 165-173
[7] Wahid, S. G., Temesgen, T. M., Optimal geometric representation of turbomachinery cascades using NURBS, *Inverse Problems in Science and Engineering*, 11(2003), 2, pp. 359-373
[8] Cheng, J., *et al*., Multi-objective optimization of incidence features for cascade, *Journal of Aerospace Power*, 32(2017), 12, pp. 3064-3072
[9] Cheng, Y., *et al*., Efficient aerodynamic optimization of turbine blade profiles: an integrated approach with novel HDSPSO algorithm, *Multidiscipline Modeling in Materials and Structures*, 20(2024), 4, pp. 725-745
[10] Georgia, N. K., *et al*., A software tool for parametric design of turbomachinery blades, *Advances in Engineering Software*, 40(2009), 1, pp. 41-51
[11] Wang, W., *et al*., Optimization design on cascade profile based on entropy generation theory. *Journal of Huazhong University of Science and Technology*, 49(2021), 9, pp. 52-58(in Chinese language)
[12] Song, P., *et al*., Blade shape optimization for transonic axial flow fan, *Journal of Mechanical Science and Technology*, 29(2015), 3, pp. 931-938(in Chinese language)
[13] Yu, J., *et al*., Adjoint optimization of multistage axial compressor blades with static pressure constraint at blade row interface, *International Journal of Turbo and Jet-Engines*, 33(2016), 2, pp. 105-118
[14] Yang, J., *et al*., Design optimization of a supersonic through-flow fan rotor based on the blade profiles, *International Journal of Turbo and Jet Engines*, 40(2023), 4, pp. 503-517
[15] Juri, B., *et al*., Numerical and Experimental Investigation of Axial Gap Variation in High-pressure Steam Turbine Stages, *Journal of Engineering for Gas Turbines and Power*, 139(2017), 5, pp. 052603

- Paper submitted: 07 June 2024
- Paper revised: 26 July 2024
- Paper accepted: 29 July 2024